# Astigmatism inducing the degenerate effect in nearly hemispherical cavities: Generation of three-dimensional structured light

J. C. Tung[a], Y. H. Hsieh [a], H. C. Liang[b], K. W. Su[a], K. F. Huang[a], and Y. F. Chen*[a]

[a] Department of Electrophysics, National Chiao Tung University, 1001 Ta-Hsueh Rd., Hsinchu 30010, Taiwan

[b] Institute of Optoelectronic Science, National Taiwan Ocean University, 2 Pei-Ning Rd., Keelung 20224, Taiwan

## Abstract

We originally perform an analytical form to explore the influence of the astigmatism on the degenerate effect in nearly hemispherical cavities. The frequency spectrum near hemispherical cavities clearly reveals that not only the difference of cavity lengths between each degeneracies but also frequency gaps have significant difference from non-hemispherical cavities. We further thoroughly demonstrate the laser experiment under the condition of nearly hemispherical cavities to confirm the theoretical exploration that the transverse topology of three-dimensional (3D) structured light in the degenerate cavities is well localized on the Lissajous curves.

**Keywords**: Lissajous curves, degenerate cavity, hemispherical cavity, orbital angular momentum

## I Introduction

The orbital angular momentum (OAM) of structured light has received significant attention over the past decades since it has given rise to many developments in optical trapping [1-4], optical tweezers [5], operation and detection of photons [6,7], imaging processing [8], producing chirality of twisted metal nanostructures [9,10], spiral interferometry [11] and astronomy [12]. One of the most interesting applications of such light beam is in the area of information transfer. The spatial modes of structured light processing OAM used as information channels carrying independent data streams for optical communication have become an interesting issue of active research in recent years [13-20]. Thus it is believed that developing the kaleidoscopic spatial modes of light with OAM is an important step in the application of communication.

In the paraxial approximation, a light field with an azimuthal phase term $\exp(il\phi)$ has an OAM of $l\hbar$ per photon along its propagation direction [21]. Therefore, the investigation of high-order structured beams is useful for developing the idea for generating large OAM. Recently, a variety of three-dimensional (3D) structured light with transverse patterns localized on the Lissajous figures has been explored from the degenerate laser resonators under the selective pumping [22-24]. More intriguingly, these 3D Lissajous structured beams formed by the coherent superposition of high-order HG eigenmodes could be converted into the corresponding LG modes. It is also verified that the optical Lissajous beams can be transformed into the optical trochoidal beams carrying huge OAM by using a $\pi/2$-cylindrical-lens mode converter [23].

To efficiently increase the order of the lasing mode under a finite range of the selective pumping, we can obtain extremely high-order Lissajous structured beams near the hemispherical cavity with the laser crystal closely approaching to the beam waist in a concave-plano resonator. For a concave-plano resonator, the hemispherical cavity is under the critical condition of the stable cavity, $L=R$, where $L$ is the cavity length, and $R$ is the curvature radius of the concave mirror. Although the Lissajous structured beams have been observed and analyzed in the non-hemispherical laser cavities [22-24], there has been no experiment and theory confirmed in nearly hemispherical cavities thus far.

In this paper we originally perform an analytical form to investigate the influence of the astigmatism on the degenerate effect in nearly hemispherical cavities. Through exploring the frequency spectrum near hemispherical cavities, it can be seen that not only the difference of cavity lengths between each degeneracies

Optical Manipulation Conference, edited by Takashige Omatsu, Ryuji Morita, Proc. of SPIE Vol. 10252, 102520G · © 2017 SPIE · CCC code: 0277-786X/17/$18 · doi: 10.1117/12.2275921

but also frequency gaps are recognizably different from non-hemispherical cavities [24]. In experiments, we use a microchip laser with a selective pumping scheme to observe the tomographic images of the 3D Lissajous structured beams near hemispherical cavities. It also has been confirmed that the spatial structures of the Lissajous beams generated from nearly hemispherical cavities can be excellently reconstructed with the present theoretical model.

## II Experimental setup for the generation of Lissajous structured beams

Here we demonstrate 3D Lissajous structured beams generated from nearly hemispherical cavities by exploiting the selective pumping in a concave-plano resonator as shown in Fig. 1. The radius of curvature of the concave mirror is $R$=10 mm and the reflectivity is 99.8% at the wavelength of 1064 nm. The gain medium is an $a$-cut 2.0-at.% $Nd^{3+}$:$YVO_4$ crystal with a length of 2 mm. One side of the gain medium is coated for antireflection at 808nm and 1064 nm (reflection < 0.1%) and the other side is coated to be an output coupler with a transmission of 0.5% at 1064 nm. The gain medium is precisely controlled to vary the cavity length. The pump source is an 808-nm fiber-coupled laser diode with a core diameter of 100 μm, a numerical aperture of 0.16, and a maximum output power of 3 W. A focusing lens with 20 mm focal length and 90% coupling efficiency is used to reimage the pump beam into the gain medium with the off-center displacements of $\Delta x$=0.25mm and $\Delta y$=0.25mm in the $x$- and $y$- directions, respectively. The pump radius is estimated to be approximately 25 μm.

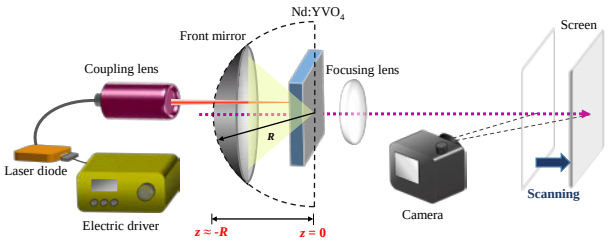


Figure 1. Experimental laser setup with the off-center selective pumping to excite 3D Lissajous structured beams for exploring the degenerate effect near hemispherical cavities.

## III Manifesting 3D Lissajous structured beams near the hemispherical cavities

Under the paraxial approximation, the wave function of eigenmodes for the laser cavity formed by a concave mirror with radius of curvature $R$ at $z$=-$L_{opt}$ and a plane mirror at $z$=0 can be divided into two waves traveling in opposite directions [24]: $\Phi_{m,n,\ell} = [\Phi^{(+)}_{m,n,\ell} - \Phi^{(-)}_{m,n,\ell}]/\sqrt{2}$, where

$$\Phi^{(\pm)}_{m,n,\ell}(x,y,z) = \psi_{m,n}(x,y,z) \times e^{\pm i\left[k_{m,n,\ell}\tilde{z} - (m+1/2)\theta_{G,x}(z) + (n+1/2)\theta_{G,y}(z)\right]}, \quad (1)$$

$$\psi_{m,n}(x,y,z) = \sqrt{(2/\pi)\Big/\left[w_x(z)w_y(z)2^{m+n}m!n!\right]} \times e^{-\frac{\tilde{x}^2+\tilde{y}^2}{2}} H_m(\tilde{x})H_n(\tilde{y}), \quad (2)$$

$H_m(\cdot)$ is the Hermite polynomial of order $m$, $k_{m,n,l} = \omega_{m,n,l}/c$ and $\omega_{m,n,l}$ is the eigen-frequency. The eigen-frequencies of the spherical cavity can be generally given by $\omega_{m,n,l} = l\omega_z + (m+1/2)\omega_{t,x} + (n+1/2)\omega_{t,y}$, where $l$ is the longitudinal mode index, $m$ and $n$ are the transverse mode indices, $\omega_z$ is the longitudinal mode spacing, and $\omega_{t,x}$ and $\omega_{t,y}$ are the transverse mode spacings in the $x$- and $y$-directions. Due to the inevitable symmetry breaking induced by the birefringence of the gain medium and the angle of the beam divergence in the cavities, the effective cavity lengths can be generally expressed as $L_{t,x}$=$L_t$+$d$/2 and $L_{t,y}$=$L_t$-$d$/2, where $L_t$ is the mean value of $L_{t,x}$ and $L_{t,y}$ given by $L_t$= $L_{cav}$+[(1/$n_r$)-1]$L_g$, and $d$ is the difference between $L_{t,x}$ and $L_{t,y}$. The frequency spectrum $\omega_{m,n,l}$ in the neighborhood of the indices ($m_o$, $n_o$, $l_o$) is given by

$$\left(\frac{\Delta\omega}{\omega_z}\right) = (m-m_o)\left(\frac{\omega_{t,x}}{\omega_z}\right) + (n-n_o)\left(\frac{\omega_{t,y}}{\omega_z}\right) + (\ell-\ell_o), \quad (3)$$

where $\Delta\omega = \omega_{m,n,l} - \omega_{mo,no,lo}$ is frequency difference. Figure 2 shows the frequency spectrum $\omega_{m,n,l}$ in the neighborhood of the indices ($m_o$, $n_o$, $l_o$) as a function of the effective cavity length in the range of 9.977mm≤ $L_t$ ≤9.995mm for $R$=10mm and $d$=10μm. To reveal the degeneracies near the hemispherical cavities, the transverse frequencies with considering the second order in the expansion of $\omega_{t,x}/\omega_z$ and $\omega_{t,y}/\omega_z$ can be derived as

$$\frac{\omega_{t,x}}{\omega_z} = \frac{1}{2} + \gamma \frac{q}{\sqrt{p^2 - q^2}} \; ; \; \frac{\omega_{t,y}}{\omega_z} = \frac{1}{2} - \gamma \frac{p}{\sqrt{p^2 - q^2}} \, . \tag{4}$$

where $\gamma = (\sqrt{d / R}) / \pi$ .

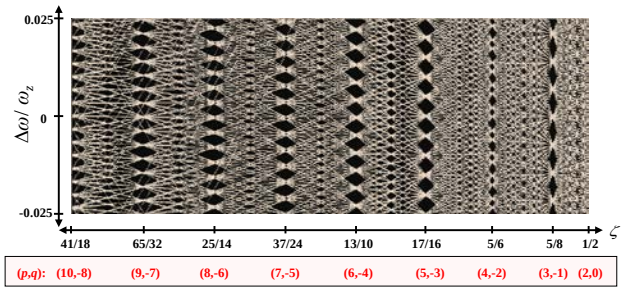


Figure 2. Frequency spectrum $\omega_{m,n,l}$ of the nearly hemispherical cavities in the neighborhood of the indices ($m_o$, $n_o$, $l_o$) as a function of the normalized cavity length $L_t / R$ for an example of $R$=10mm and $d$=10μm

Considering the 2$N$+1 excited modes and a selective pumping with the off-center displacements $\Delta x$ and $\Delta y$ in the $x$- and $y$-directions, the wave function of degenerate laser modes can be expressed as $\Psi = [\Psi^{(+)} - \Psi^{(-)}] / \sqrt{2}$ , where

$$\Psi^{(\pm)}(x, y, z) = \sum_{u=-N}^{N} c_{m,n,\ell} \, \Phi^{(\pm)}_{m,n,\ell}(x, y, z) \, , \tag{5}$$

$c_{m,n,l}$ is the amplitude coefficient, $m$=$m_o$+$pu$, $n$=$n_o$+$qu$, $l$=$l_o$+$su$, $m_o$ =[$\Delta x / w_x(z_c)$]$^2$, and $n_o$ =[$\Delta y / w_y(z_c)$]$^2$, and $z_c$ is the location of the gain medium. Through the spatial overlap between the transverse eigenmode and the pump source with the Gaussian distribution [32], the coefficients $c_{m,n,l}$ can be derived as $c_{m,n,\ell} = \left[ (m_o)^{m/2} (n_o)^{n/2} e^{-(m_o + n_o)/2} \Big/ \sqrt{m!\, n!} \right] \Big/ (2N+1)$ . With the degenerate conditions given by Eq. (4), the intensity distribution $|\Psi(x,y,z)|^2$ depicted in Figure 3 for various ($p$,$q$) can be found to correspond to the 3D geometric surface with the transverse topology of Lissajous curves with the parameters of $m_o$=$n_o$=40, $R$=10mm and $d$=0.25mm. The experimentally tomographic images of the lasing modes are also shown in Fig. 3. The tomographic images of the lasing modes are obtained by controlling the exposure time of the camera to selectively capture the transverse patterns inside the cavity along the longitudinal propagation. Moreover, a focusing lens is used to reimage the lasing modes onto a paper screen that is moved by tracking the camera to record the tomographic images. The transverse patterns can be clearly seen to be localized on the Lissajous curves in Fig. 3.

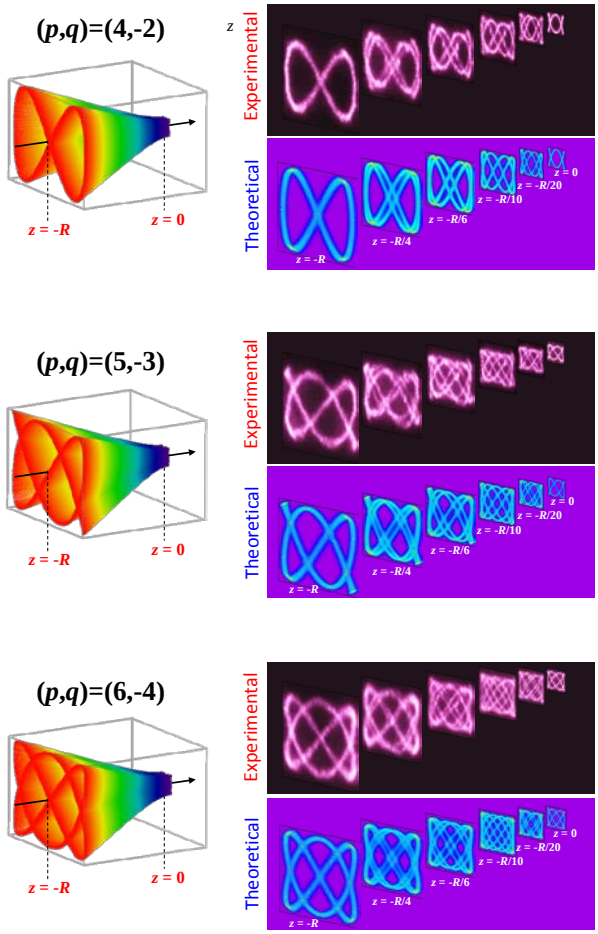


Figure 3. Numerical and experimental results for the tomographic images of Lissajous structured beams inside the cavity for various ($p$,$q$) with the parameters of $m_o$=$n_o$=40, $R$=10mm and $d$=0.25 mm.

## VI Conclusions

In summary, we have theoretically confirmed the influence of the astigmatism on the degenerate effect in nearly hemispherical cavities. Through theoretical analysis of the frequency spectrum, it has been manifested that the difference of cavity lengths between each

degeneracies is decreased with the cavity length approaching to the hemispherical cavity, and a large frequency gap can be related to the degeneracy with a simple integer pair (*p*,*q*). For verifying the theoretical exploration of the 3D Lissajous structured beams in the degenerate cavities, we have employed a microchip laser with the selective pumping scheme to observe the tomographic images of the structured beams near hemispherical cavities.

## References


[1] K. T. Gahagan and G. A. Swartzlander Jr., "Optical vortex trapping of particles," Opt. Lett. **21**(11), 827–829 (1996).

[2] M. Dienerowitz, M. Mazilu, P. J. Reece, T. F. Krauss, and K. Dholakia, "Optical vortex trap for resonant confinement of metal nanoparticles," Opt. Express **16**(7), 4991–4999 (2008).

[3] H. He, M. E. J. Friese, N. R. Heckenberg, and H. Rubinsztein-Dunlop, "Direct observation of transfer of angular momentum to absorptive particles from a laser beam with a phase singularity," Phy. Rev. Lett. **75**, 826 (1995).

[4] D. G. Grier, "A revolution in optical manipulation," Nature **424**, 810-816 (2003).

[5] M. Padgett and R. Bowman, "Tweezers with a twist," Nature Photon. **5**, 343–348 (2011).

[6] D. Akamatsu and M. Kozuma, "Coherent transfer of orbital angular momentum from an atomic system to a light field," Phys. Rev. A **67**, 023803 (2003).

[7] J. Leach, M. J. Padgett, S. M. Barnett, S. Franke-Arnold, and J. Courtial, "Measuring the orbital angular momentum of a single photon," Phy. Rev. Lett. **88**, 257901 (2002).

[8] S. Bernet, A. Jesacher, S. Fürhapter, C. Maurer and M. Ritsch-Marte, "Quantitative imaging of complex samples by spiral phase contrast microscopy." Opt. Express **14**(9), 3792–3805 (2006).

[9] K. Toyoda, K. Miyamoto, N. Aoki, R. Morita, and T. Omatsu, "Using optical vortex to control the chirality of twisted metal nanostructures," Nano Letters **12**(7), 3645–3649 (2012).

[10] K. Toyoda, F. Takahashi, S. Takizawa, Y. Tokizane, K. Miyamoto, R. Morita, and T. Omatsu, "Transfer of light helicity to nanostructures," Phys. Rev. Lett. **110**, 143603 (2013).

[11] A. Jesacher, S. Fürhapter, S. Bernet, and M. R. Marte, "Spiral interferogram analysis," J. Opt. Soc. Am. A **23**(6), 1400-1409 (2006).

[12] N. M. Elias II, "Photon orbital angular momentum in astronomy." Astron. Astrophys. **492**, 883–922 (2008).

[13] G. Li and X. Liu, "Focus issue: space multiplexed optical transmission," Opt. Express, **19**(17), 16574-16575 (2011).

[14] S. Randel, R. Ryf, A. Sierra, P. J. Winzer, A. H. Gnauck, C. A. Bolle, R. Essiambre, D. W. Peckham, A. McCurdy, and R. Lingle, "6×56-Gb/s mode-division multiplexed transmission over 33-km few-mode fiber enabled by 6×6 MIMO equalization, " Opt. Express, **19**(17), 16697-16707 (2011).

[15] J. Wang, J. Y. Yang, I. M. Fazal, N. Ahmed, Y. Yan, H. Huang, Y. Ren, Y. Yue, S. Dolinar, M. Tur and A. E. Willner, "Terabit free-space data transmission employing orbital angular momentum multiplexing, " Nature Photon. **6**, 488-496 (2012).

[16] Y. Ding, J. Xu, F. D. Ros, B. Huang, H. Ou, and C. Peucheret, "On-chip two-mode division multiplexing using tapered directional coupler-based mode multiplexer and demultiplexer, " Opt. Express, **21**(8), 10376-10382 (2013).

[17] L. W. Luo, N. Ophir, C. P. Chen, L. H. Gabrielli, C. B. Poitras, K. Bergmen and M. Lipson "WDM-compatible mode-division multiplexing on a silicon chip, " Nat. Commun. **5**, 3069 (2014).

[18] G. Milione, M. P. J. Lavery, H. Huang, Y. Ren, G. Xie, T. A. Nguyen, E. Karimi, L. Marrucci, D. A. Nolan, R. R. Alfano, and A. E. Willner, "4 × 20 Gbit/s mode division multiplexing over free space using vector modes and a q-plate mode (de)multiplexer, " Opt. Lett., **40**(9), 1980-1983 (2015).

[19] G. Milione, T. A. Nguyen, J. Leach, D. A. Nolan, and R. R. Alfano, "Using the nonseparability of vector beams to encode information for optical communication," Opt. Lett., **40**(21), 4887-4890 (2015).

[20] H. Huang, G. Milione, M. P. J. Lavery, G. Xie, Y. Ren, Y. Cao, N. Ahmed, T. A. Nguyen, D. A. Nolan, M. J. Li, M. Tur, R. R. Alfano and A. E. Willner, "Mode division multiplexing using an orbital

angular momentum mode sorter and MIMO-DSP over a graded-index few-mode optical fibre, ” Sci. Rep. **5**, 14931 (2015).

[21] J. F. Nye and M. V. Berry, “Dislocations in wave trains,” Proc. R Soc. Lond. A **336**, 165-194 (1974).

[22] Y. F. Chen, T. H. Lu, K. W. Su, and K. F. Huang, “Devil’s staircase in three-dimensional coherent waves localized on Lissajous parametric surfaces,” Phys. Rev. Letts. **96**, 213902 (2006).

[23] Y. F. Chen, Y. C. Lin, K. F. Huang and T. H. Lu “Spatial transformation of coherent optical waves with orbital morphologies,” Phys. Rev. A **82**, 043801 (2010).

[24] J. C. Tung, P. H. Tuan, H. C. Liang, K. F. Huang and Y. F. Chen “Fractal frequency spectrum in laser resonators and three-dimensional geometric topology of optical coherent waves, ” Phys. Rev. A **94**, 023811 (2016).